Prograde and retrograde terms of gravimetric polar motion excitation estimates from the newest GRACE gravity field models

Jolanta Nastula and Justyna Śliwińska

Space Research Centre, Polish Academy of Sciences

Journees 2019, 7-9 October 2019, Paris

Introduction

- Polar motion (PM) is affected by a wide range of processes with different temporal variability. For time scales of a few years or less, the main contributors to variation in Earth's rotation are angular momentum changes caused by mass redistribution in the Earth's surficial fluids (atmosphere, ocean, land hydrosphere).
- The role of atmospheric and oceanic mass distribution on the global balance of Earth's angular momentum, described as atmospheric and oceanic angular momentum (AAM and OAM, respectively), has been well established.
- However, the role of continental hydrosphere, referred to as **hydrological angular momentum (HAM)** and obtained from different hydrological models exhibit visible discrepancies, both with respect to each other and with respect to the hydrological signal in observed PM excitation, derived from precise geodetic measurements.
- The main reason of discrepancies between diverse models estimations of HAM are differences in meteorological model forcing data, processing algorithms, temporal and spatial resolution or number of parameters estimated.
- Disagreement with observed PM data is caused by the lack of some water storage components or unrealistic simulations of other variables. Additionally, other geophysical effects, such as earthquake-induced co- and post-seismic deformations or Earth's core-mantle coupling are usually not considered in a rigorous way.

Introduction

- Alternative information on PM excitation due to global mass redistribution can be obtained from observations of temporal changes in the gravity field, provided by the **Gravity Recovery and Climate Experiment (GRACE)** mission.
- After removing tidal effects as well as non-tidal atmospheric and oceanic contributions from the GRACE-based gravity coefficients, the remaining signal is mostly an indication of the land hydrosphere (but also barystatic sea-level contributions and earthquake signatures).
- Recently, new GRACE solutions (RL06) have been developed and made available to the scientific community by the official GRACE data centres at GeoForschungsZentrum (GFZ) in Potsdam, Germany; Center for Space Research (CSR) in Austin, USA; and the Jet Propulsion Laboratory (JPL) in Pasadena, USA. However, during the 15 years of the mission, new centres also joined the network, e.g. Graz University of Technology, Austria and the Centre National d'Etudes Spatiales in Toulouse.
- First attempts to validate these solutions with respect to the observed PM excitation have been made in recent works which showed that with the newly-processed GRACE data, the consistency between particular solutions and agreement with reference data has increased. However, a full agreement between GRACE-based and observed hydrological excitation still has not been achieved.

Motivation and objectives

- A common method to describe PM excitation is either the use of two equatorial components of this function, χ_1 (along the Greenwich Meridian) and χ_2 (along 90°E), or their complex form ($\chi_1 + i\chi_2$).
- However, the polar motion excitation exhibits two circular terms: **retrograde** (clockwise) and **prograde** (counter-clockwise).
- In previous works, the Earth's PM excitation was generally decomposed into prograde and retrograde terms but at one fixed frequency. Usually, seasonal oscillations (annual, semi-annual or ter-annual) were the subject of interest, and pro- and retrograde seasonal variations were represented by their amplitudes and phases.
- Here, we are interested in the total prograde (χ_P) and retrograde (χ_R) parts of PM excitation function. We reconstruct these terms in time domain from χ_1 and χ_2 with the use of **Complex Fourier Transform.**

Motivation and objectives

- The objective of this study is to consider what the new GRACE RL06 solutions might contribute to the understanding of residual PM excitations as observed by space geodesy techniques.
- Here, we validate the gravimetric PM excitation estimates from the new GRACE solutions using observed PM excitation (geodetic residuals).
- The GRACE estimations of PM excitation are also compared to the HAM from Land Surface Discharge Model (LSDM), with consideration of effects of barystatic sea-level changes due to inflow of continental water into the oceans (sea-level angular momentum, SLAM).
- **In contrast to the previous works, here, the equatorial components of PM excitation functions (χ_1 and χ_2) are decomposed into prograde and retrograde (χ_P and χ_R) terms by applying Complex Fourier Transform method.** The prograde and retrograde terms of PM excitation are also separated into seasonal and non-seasonal oscillations.

Data

I. Data used for determination of hydrological signal in observed (geodetic) PM excitation function (geodetic residuals, GAO) – **reference series**

II. Data used for determination od hydrological excitation functions (HAM) – **evaluated series**

Data

used for determination of geodetic residuals (GAO)

- The observed geodetic PM excitation function **(Geodetic Angular Momentum, GAM)** can be computed from observed coordinates of the Earth's pole, provided by the SLR, VLBI, GNSS techniques.
- To obtain hydrological signal in this excitation, the impacts of **atmosphere (Atmospheric Angular Momentum, AAM)** and **ocean (Oceanic Angular Momentum, OAM)** should be removed, using geophysical models:

$$\mathrm{GAO} = \mathrm{GAM} - [\mathrm{AAM}_{mass} + \mathrm{AAM}_{motion} + \mathrm{OAM}_{mass} + \mathrm{OAM}_{motion}],$$

where:

AAM_{mass} is related to the impact of atmospheric pressure,

AAM_{motion} is related to the impact of wind speed,

OAM_{mass} is related to the impact of ocean bottom pressure,

OAM_{motion} is related to the impact of ocean currents.

Data

used for determination of geodetic residuals (GAO)

1) **Geodetic Angular Momentum (GAM)** – χ_1 and χ_2 components of observed geodetic PM excitations, obtained from the time series of the Earth Orientation Parameters (EOP C04) and provided by the International Earth Rotation and Reference System Service (IERS) (https://www.iers.org/);
2) **mass term of AAM + OAM** – χ_1 and χ_2 components of joint AAM and OAM, computed from ΔC_{21}, ΔS_{21} coefficients of the average non-tidal atmosphere and ocean de-aliasing model time series **GRACE GAC JPL RL06** (ftp://podaac-ftp.nasa.gov/);
3) **motion term of AAM** – χ_1 and χ_2 components for motion term of AAM computed from European Centre for Medium-range Weather Forecasts (**ECMWF**) and provided by the GFZ;
4) **motion term of OAM** – χ_1 and χ_2 components for motion term of OAM, computed from Max Planck Institute Ocean Model (**MPIOM**) and provided by the GFZ.

GAO = GAM (IERS) – [**AAM+OAM mass term computed from GAC JPL RL06** +
+ **AAM motion term obtained from GFZ (ECMWF)** +
+ **OAM motion term obtained from GFZ (MPIOM)**]

Data

used for determination of hydrological excitation functions (HAM)

1) Time series of ΔC_{21}, ΔS_{21} from the monthly **GRACE satellite-only models (GSM)** from the following solutions:

Old		New	
CSR RL05	and	**CSR RL06**	– Center for Space Research, Austin, U.S.A.
JPL RL05	and	**JPL RL06**	– Jet Propulsion Laboratory, Pasadena, U.S.A.
GFZ RL05	and	**GFZ RL06**	– GeoforschungsZentrum, Potsdam, Germany
ITSG 2016	and	**ITSG 2018**	– Graz University of Technology, Austria
CNES RL03	and	**CNES RL04**	– Centre National d'Études Spatiales, Toulouse, France

2) χ_1 and χ_2 components of HAM computed from **Land Surface Discharge Model (LSDM)**, and χ_1 and χ_2 components of **Sea-Level Angular Momentum (SLAM)**, both calculated by the GFZ and accessed from ftp://esmdata.gfz-potsdam.de/EAM. Here, we consider the sum of HAM and SLAM and call it LSDM.

Methodology

HAM computation

1) The χ_1, χ_2 components of PM excitation from GRACE observations were estimated from ΔC_{21}, ΔS_{21} coefficients using the formulas (*Gross, 2015*):

$$\chi_1 = -\sqrt{\frac{5}{3}} \cdot \frac{1.608 \cdot R_e^2 \cdot M}{C - A'} \Delta C_{21},$$

$$\chi_2 = -\sqrt{\frac{5}{3}} \cdot \frac{1.608 \cdot R_e^2 \cdot M}{C - A'} \Delta S_{21},$$

where ΔC_{21} and ΔS_{21} are the Stokes coefficients of the Earth's gravity field; R_e and M are the Earth's mean Earth's radius (6378136.6 m) and mass (5.9737×10^{24} kg), respectively; A = 8.0101×10^{37} kg·m^2, B = 8.0103×10^{37} kg·m^2, and C = 8.0365×10^{37} kg·m^2 are the Earth's principal moments of inertia, and A' = (A+B)/2 is the average of the equatorial Earth's principal moments of inertia (Table 1 in *Gross, 2015*).

2) The χ_1, χ_2 components of HAM from LSDM and SLAM were taken directly from ftp://esmdata.gfz-potsdam.de/EAM.

Methodology

Time series processing

1) Time series were **interpolated** into the same period (between January 2003 and December 2015);
2) Due to different sampling resolution of the data sources (24 h for GAM, 3 h for ECMWF and MPIOM models, and only monthly for GRACE), all series were **downsampled to monthly time-steps using Gaussian filter;**
3) To calculate **seasonal oscillations**, the linear trends were first removed from the time series. Then, the seasonal components were calculated by fitting the seasonal model using the least squares method. The fitted model included a sum of sinusoids with the periods of 1, 1/2 and 1/3 year;
4) The **non-seasonal changes** were obtained after removing linear trends and seasonal model from the series;
5) The **prograde and retrograde terms** of PM excitation function were computed using **Complex Fourier Transform** method (*Bizouard, 2016*);
6) The non-seasonal prograde and retrograde terms of PM excitation function were separated into **short-term (periods <720 days)** and **long-term (periods >720 days) oscillations** using higher-order 8-pole sine wave Butterworth filter.

Methodology

Complex Fourier Transform

- To compute prograde and retrograde oscillations in PM excitation, the separation of the forward (+) and backward (–) terms is required.
- **Complex Fourier Transform** enable to determine retrograde and prograde circular terms of the PM excitation. The total prograde and retrograde parts of these excitations are reconstructed in time domain.
- Over a given time interval, complex coordinates of the equatorial excitation can be decomposed into complex Fourier series as follows (*Bizouard, 2016*):

$$\chi(t) = \sum_{\sigma > 0} a_{\sigma}^{+} \mathrm{e}^{\mathrm{i}\sigma t} + \sum_{\sigma > 0} a_{\sigma}^{-} \mathrm{e}^{-\mathrm{i}\sigma t} + \chi_0 \, ,$$

where a_{σ}^{+} is the complex amplitude of the prograde term of angular frequency σ, a_{σ}^{-} is the complex amplitude of retrograde term of the same frequency; χ_0 is a constant term.

Methodology

Complex Fourier Transform

- In time domain, prograde and retrograde terms at a given frequency are determined by:

$$\chi_{\sigma}^{+}(t) = a_{\sigma}^{+} \mathrm{e}^{\mathrm{i}\sigma t} = A_{\sigma}^{+} \mathrm{e}^{\mathrm{i}\Phi_{\sigma}^{+}} \mathrm{e}^{\mathrm{i}\sigma t}, \qquad \chi_{\sigma}^{-}(t) = a_{\sigma}^{-} \mathrm{e}^{-\mathrm{i}\sigma t} = A_{\sigma}^{-} \mathrm{e}^{\mathrm{i}\Phi_{\sigma}^{-}} \mathrm{e}^{-\mathrm{i}\sigma t},$$

where A_{σ}^{+}, A_{σ}^{-} and Φ_{σ}^{+}, Φ_{σ}^{-} express amplitudes and phases, respectively.

- The total prograde and retrograde components in time domain can be determined by adding the individual frequency terms of the Fourier decomposition:

$$\chi^{+}(t) = \sum_{\sigma > 0} a_{\sigma}^{+} e^{i\sigma t}; \quad \chi^{-}(t) = \sum_{\sigma > 0} a_{\sigma}^{-} e^{-i\sigma t}$$

Results

Results

1) **Time series comparisons**
- ❑ non-seasonal oscillations
  - non-separated
  - separated into long-term and short-term oscillations
- ❑ seasonal oscillations

2) **Correlations with GAO and relative explained variances**
- ❑ non-seasonal oscillations
  - non-separated
  - separated into long-term and short-term oscillations
- ❑ seasonal oscillations

Time series comparisons

Seasonal oscillations

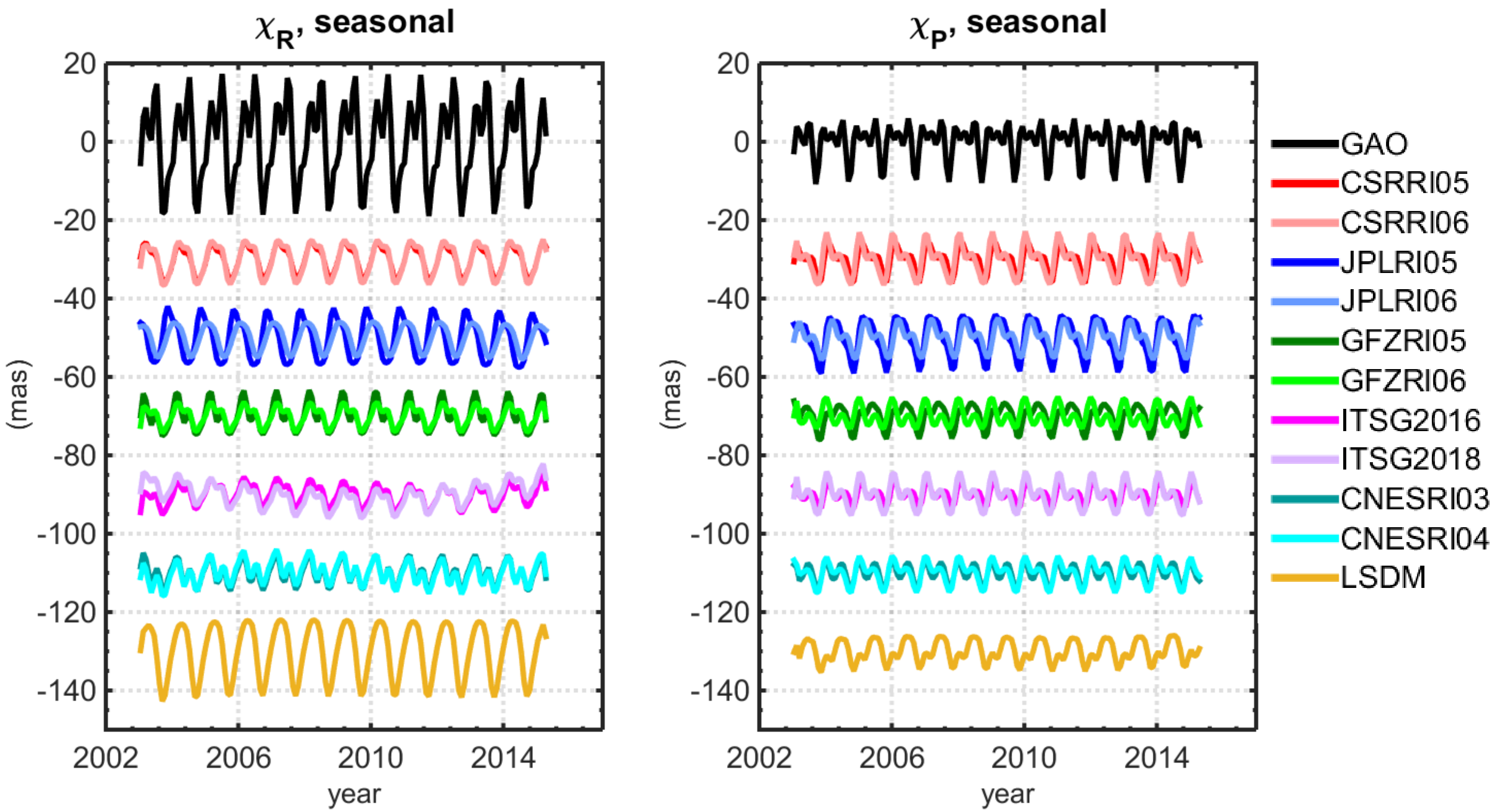

Fig. 1. Retrograde and prograde parts of seasonal variation in GAO, HAM computed from different GRACE solutions and HAM from LSDM model (with SLAM added)

Seasonal oscillations

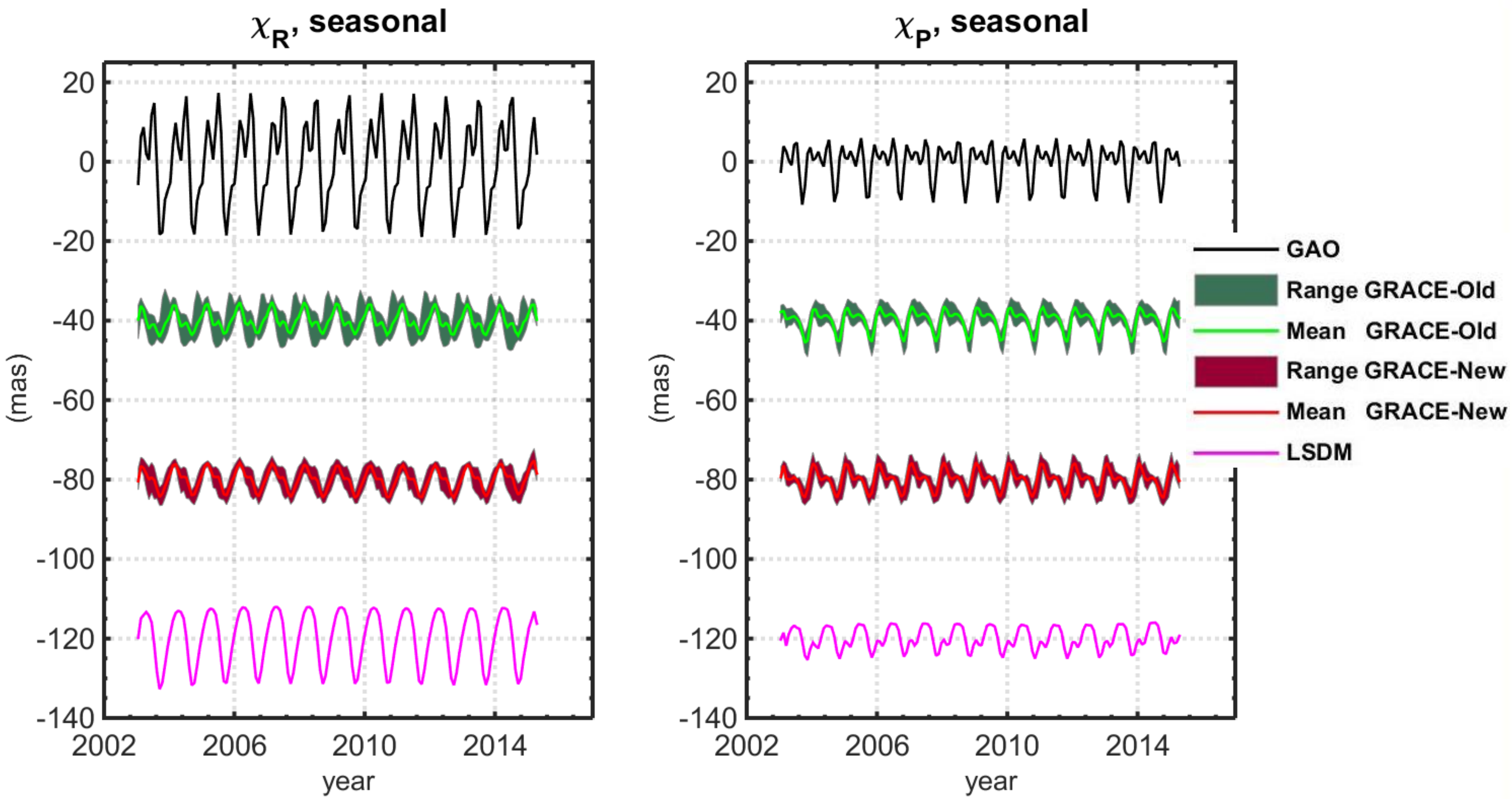

Fig. 2. Comparison of mean value with ranges between minimum and maximum for retrograde and prograde parts of seasonal variation in HAM for old and new GRACE solutions separately. Time series of GAO and HAM from LSDM model (with SLAM added) were added for comparison

Non-seasonal oscillations

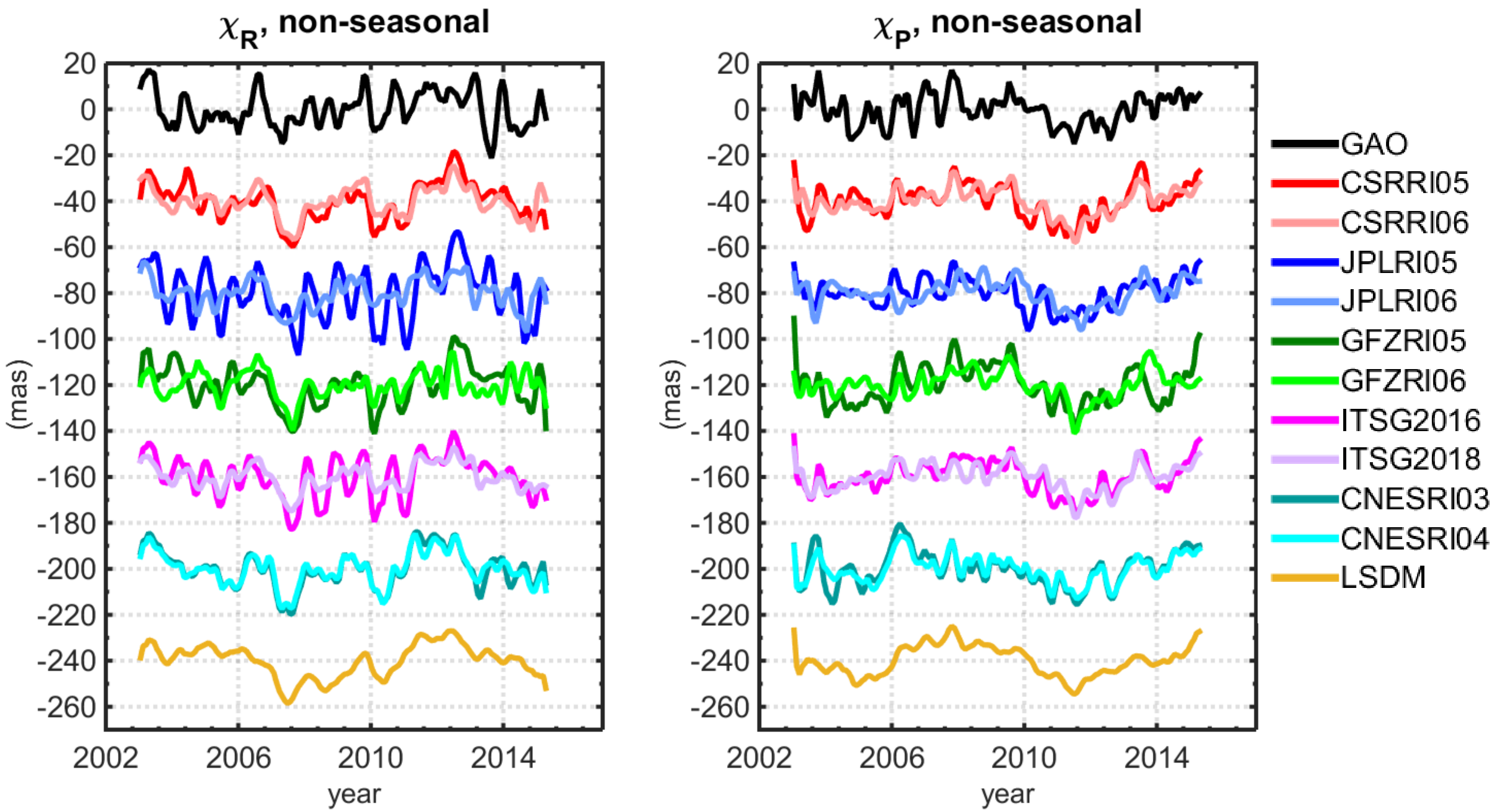

Fig. 3. Retrograde and prograde parts of non–seasonal variation in GAO, HAM computed from different GRACE solutions and HAM from LSDM model (with SLAM added)

Non-seasonal oscillations

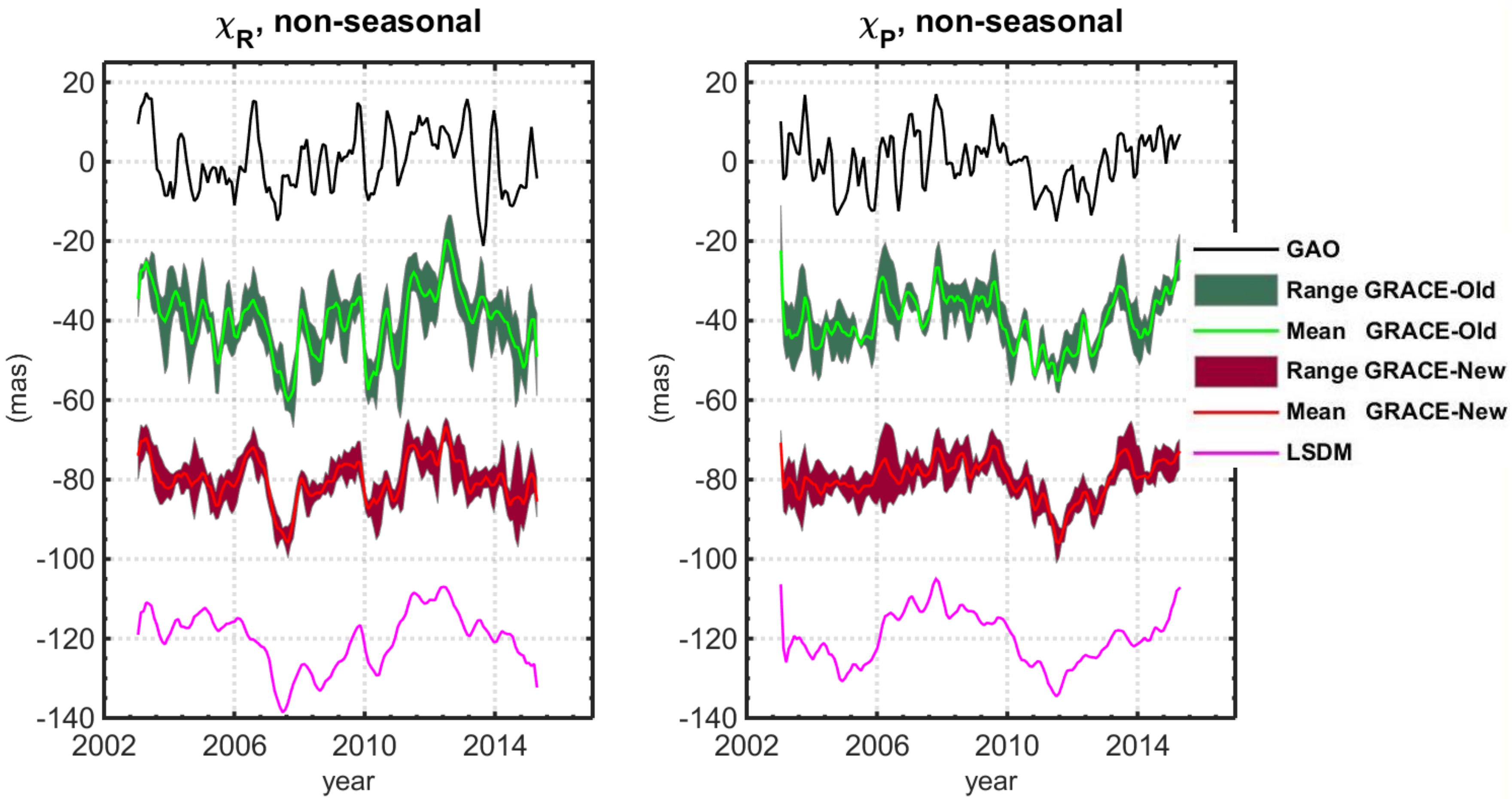

Fig. 4. Comparison of mean value with ranges between minimum and maximum for retrograde and prograde parts of non–seasonal variation in HAM for old and new GRACE solutions separately. Time series of GAO and HAM from LSDM model (with SLAM added) were added for comparison

Non-seasonal short-term oscillations

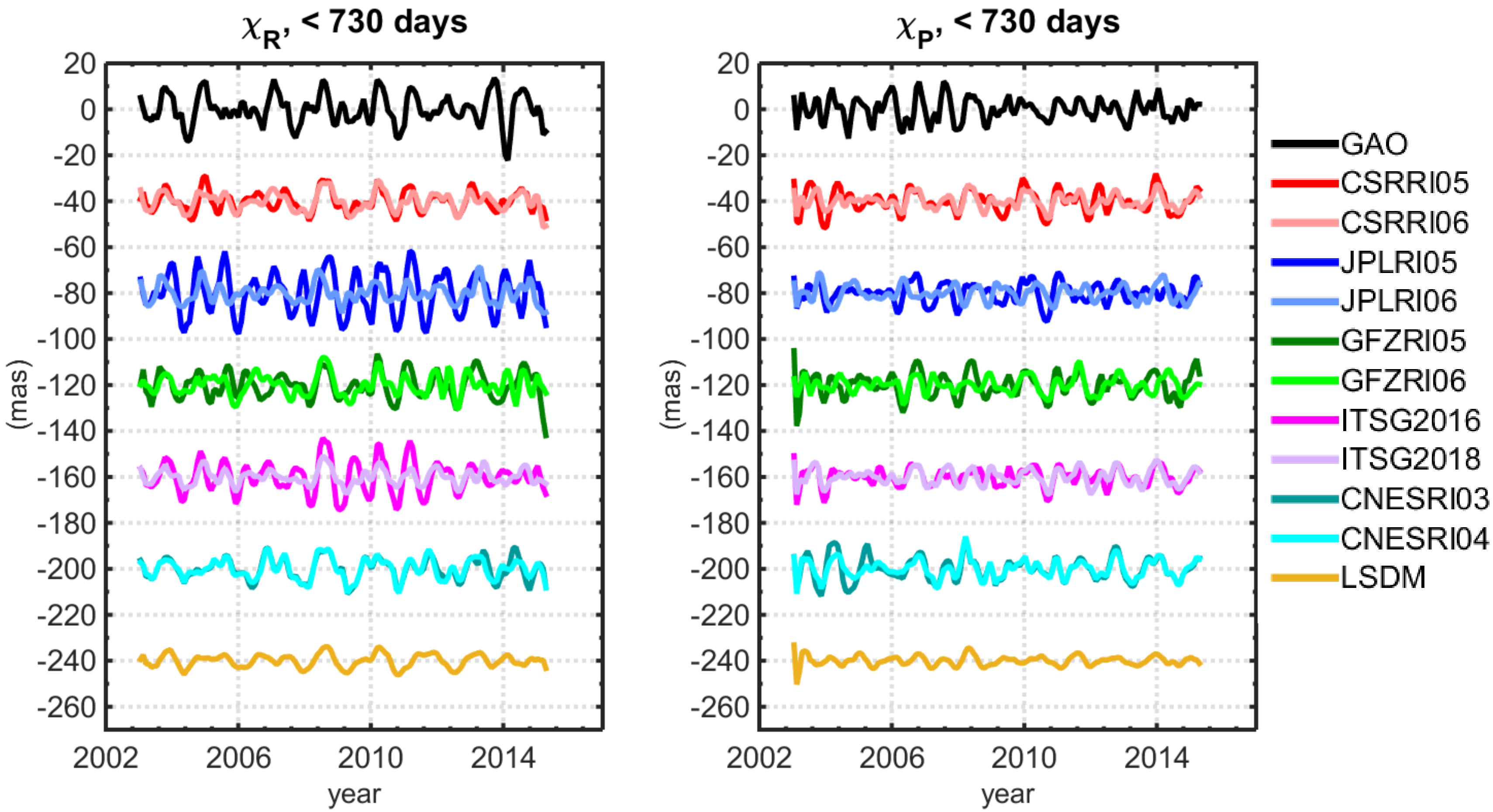

Fig. 5. Retrograde and prograde parts of short–term (periods <730 days) non–seasonal variation in GAO, HAM computed from different GRACE solutions and HAM from LSDM model (with SLAM added)

Non-seasonal short-term oscillations

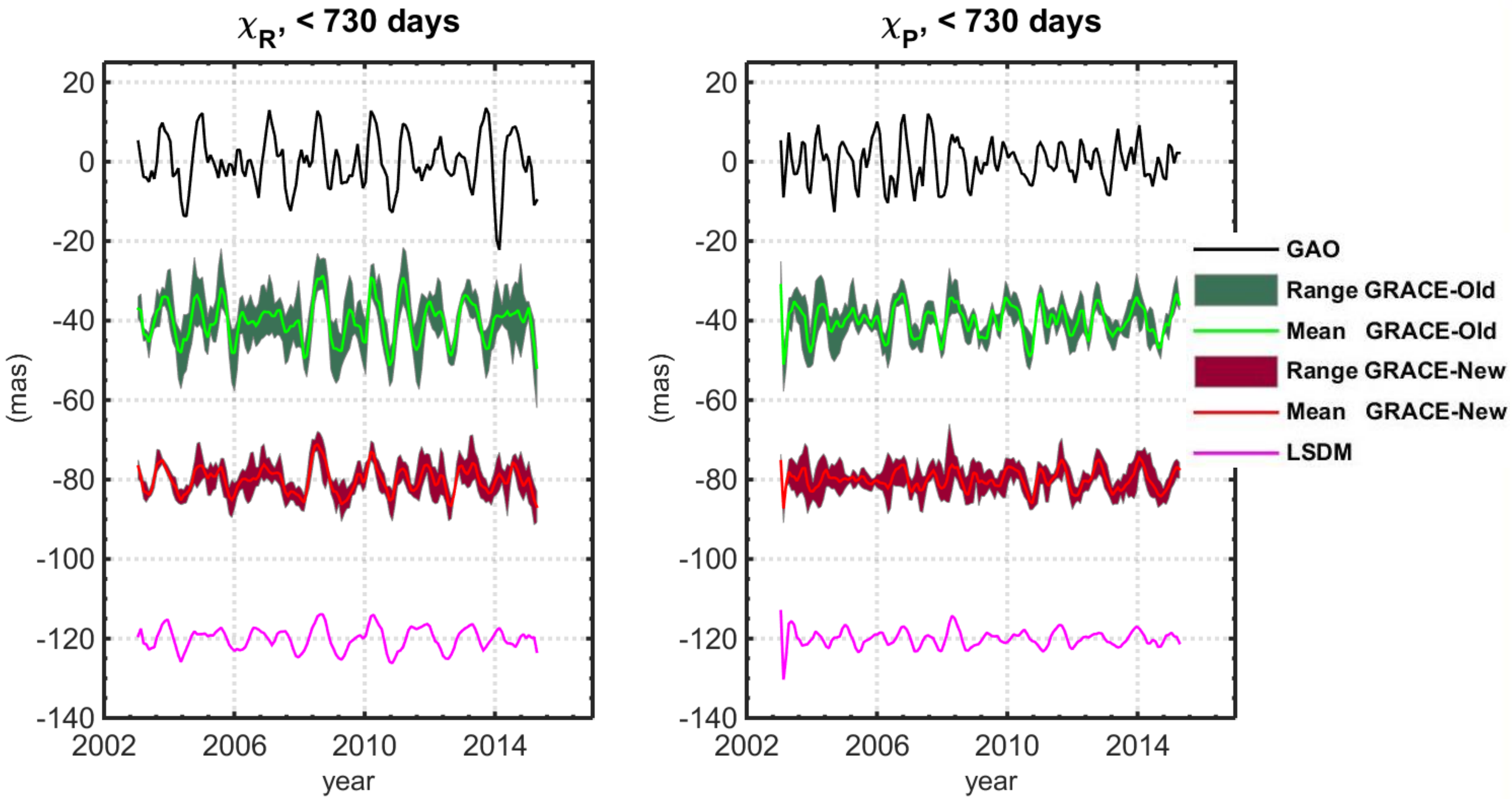

Fig. 6. Comparison of mean value with ranges between minimum and maximum for retrograde and prograde parts of short–term (periods <730 days) non–seasonal variation in HAM for old and new GRACE solutions separately. Time series of GAO and HAM from LSDM model (with SLAM added) were added for comparison

Non-seasonal long-term oscillations

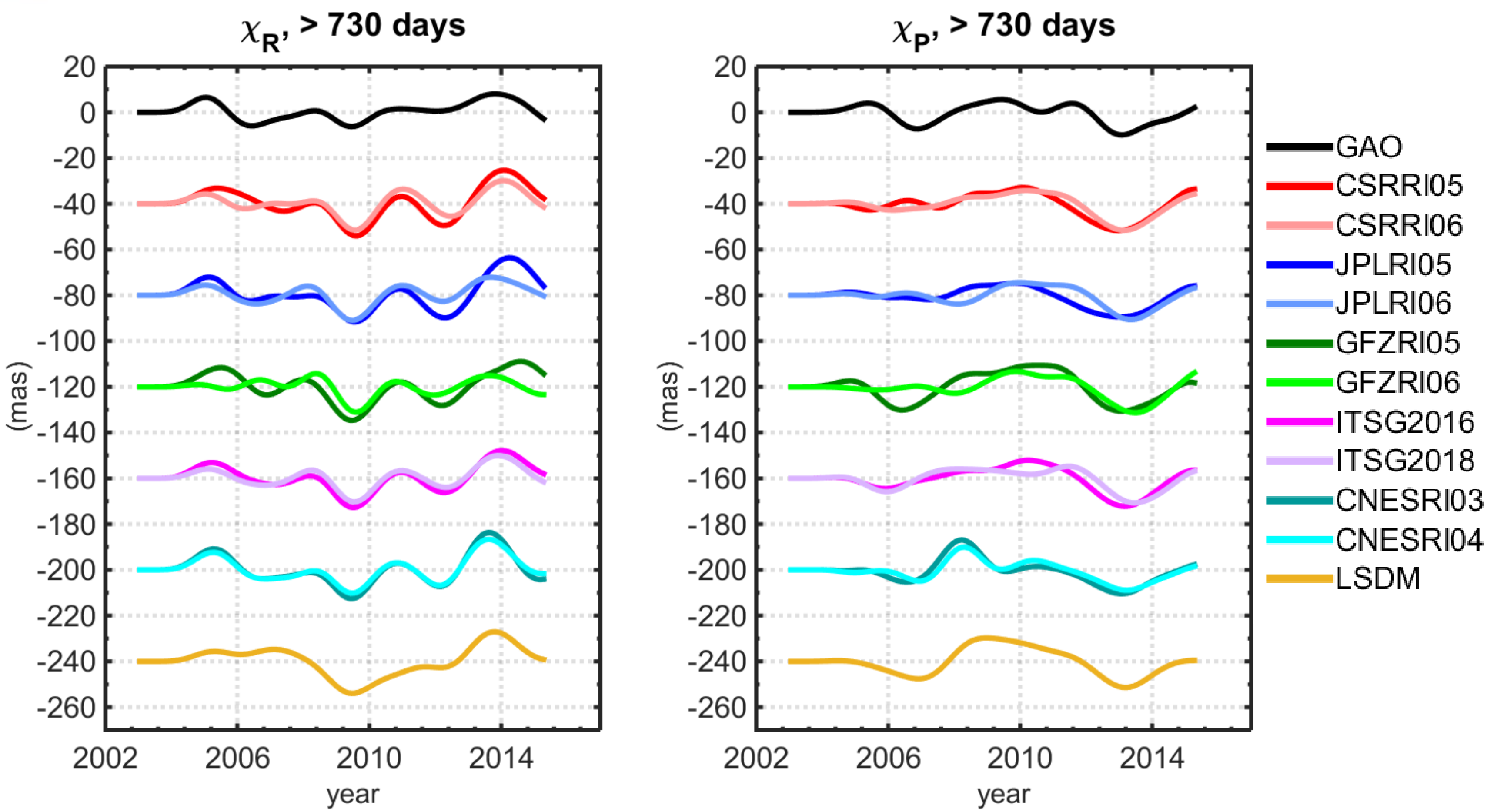

Fig. 7. Retrograde and prograde parts of long–term (periods >730 days) non–seasonal variation in GAO, HAM computed from different GRACE solutions and HAM from LSDM model (with SLAM added)

Non-seasonal long-term oscillations

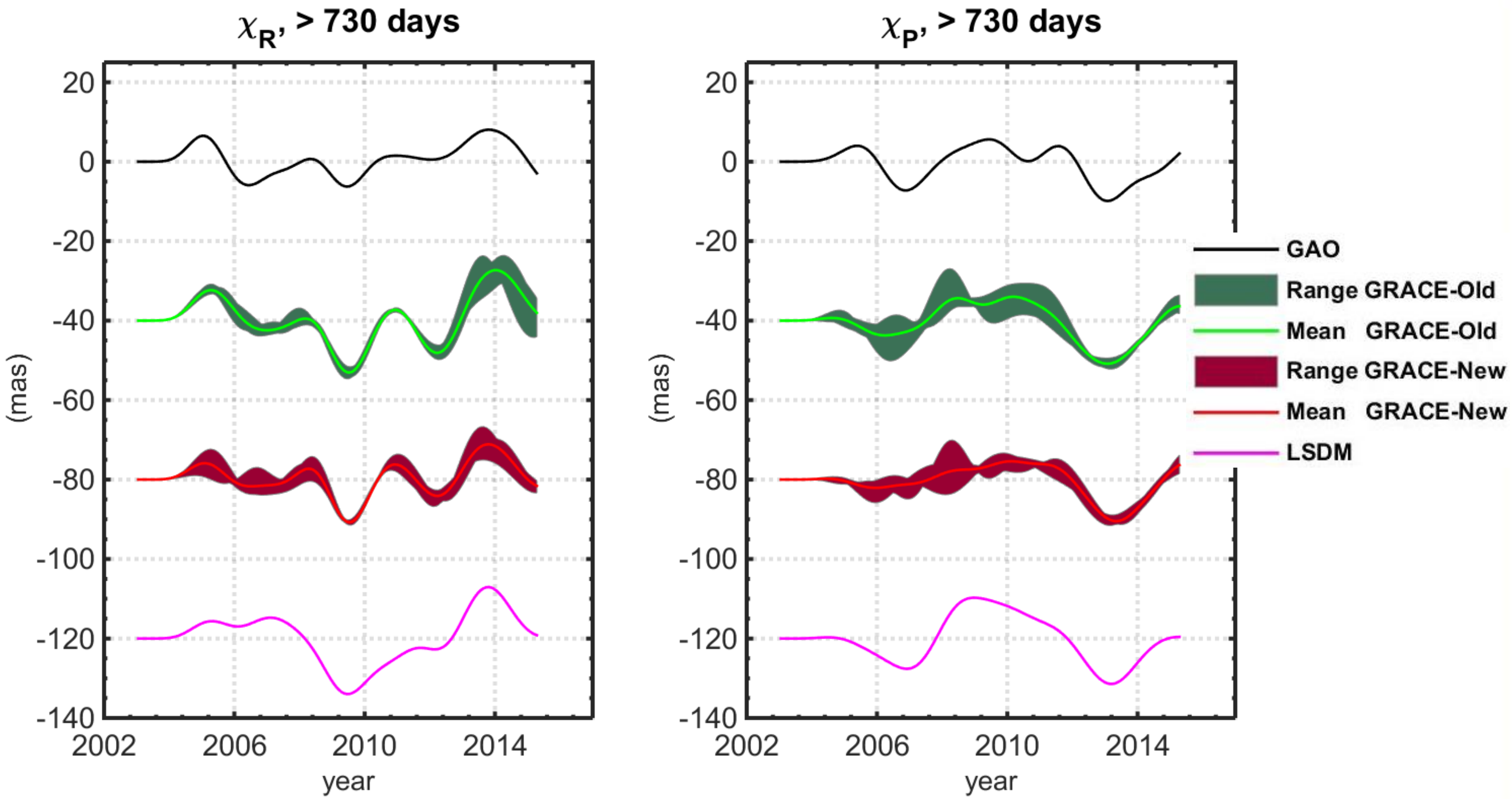

Fig. 8. Comparison of mean value with ranges between minimum and maximum for retrograde and prograde parts of long–term (periods >730 days) non–seasonal variation in HAM for old and new GRACE solutions separately. Time series of GAO and HAM from LSDM model (with SLAM added) were added for comparison

Correlations with GAO and relative explained variances

Seasonal oscillations

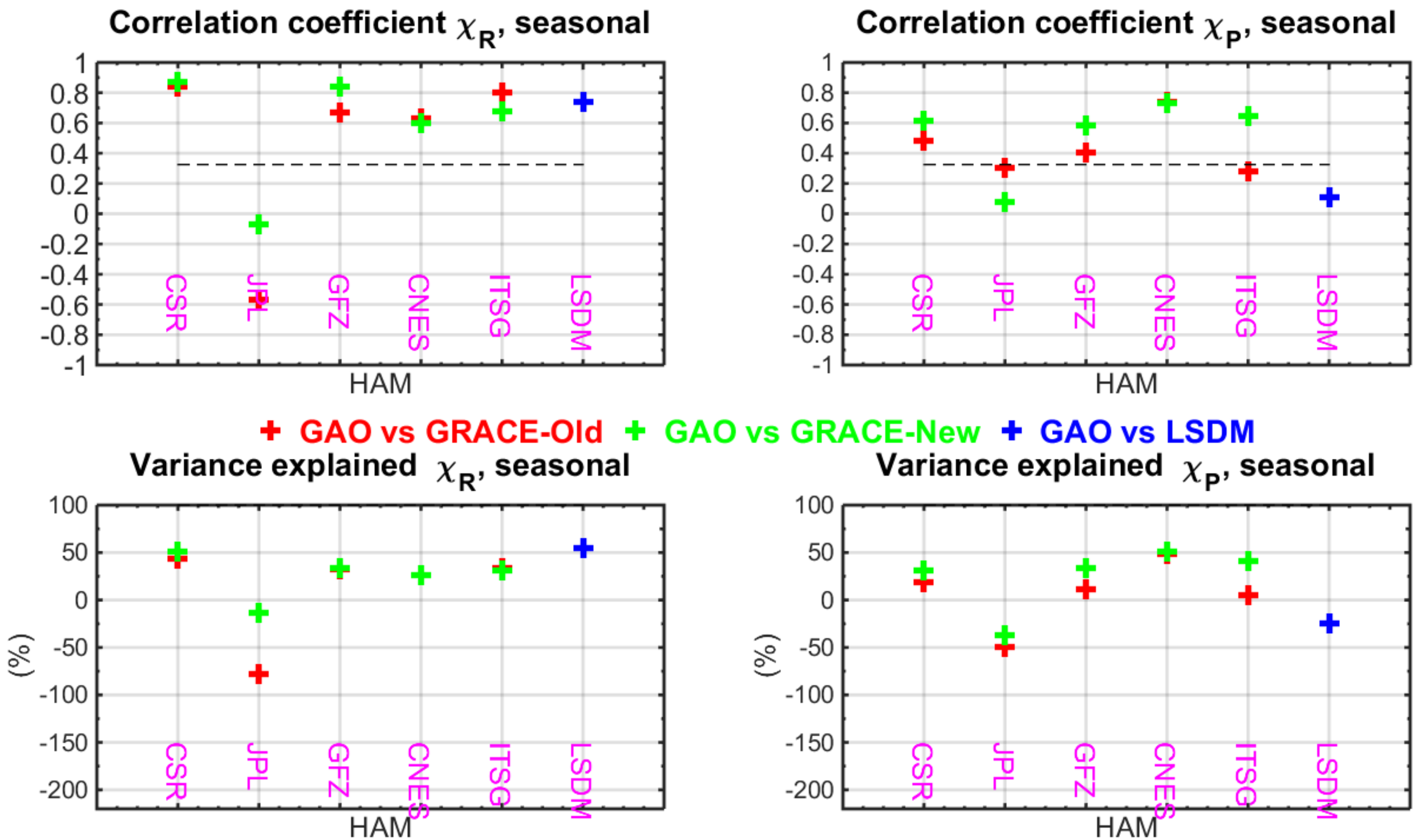

Fig. 9. Correlation coefficients of retrograde and prograde parts of seasonal variation between GAO and HAM computed from GRACE solutions and LSDM model (with SLAM added); percentage of variance in GAO explained by HAM functions. The critical value of the correlation coefficient for 25 independent points and a confidence level of 0.95 is equal to 0.34. A standard error of a difference between two correlation coefficients for 25 independent points is equal to 0.30

Non-seasonal oscillations

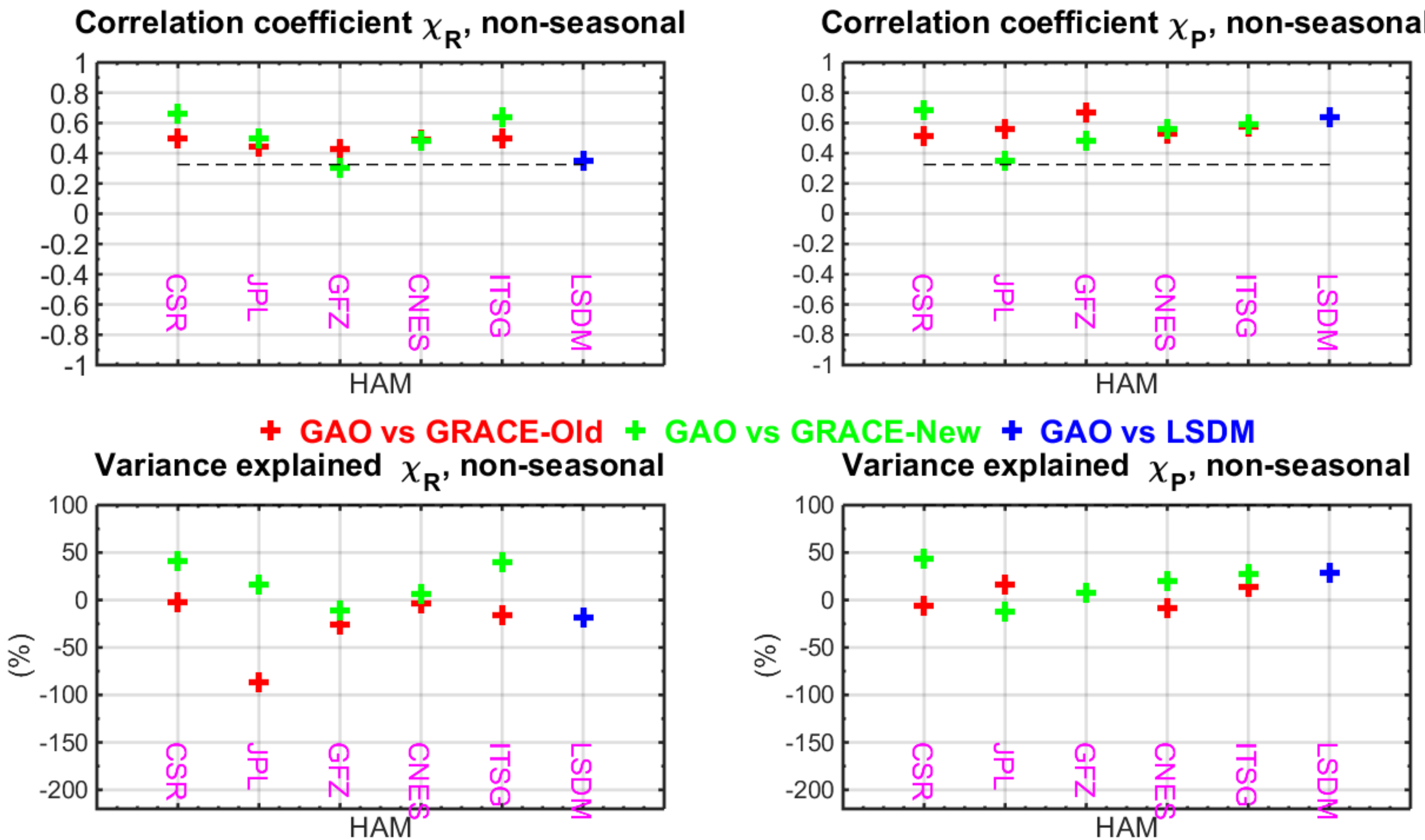

Fig. 10. Correlation coefficients of retrograde and prograde parts of non–seasonal variation between GAO and HAM computed from GRACE solutions and LSDM model (with SLAM added); percentage of variance in GAO explained by HAM functions. The critical value of the correlation coefficient for 25 independent points and a confidence level of 0.95 is equal to 0.34. A standard error of a difference between two correlation coefficients for 25 independent points is equal to 0.30

Non-seasonal short-term oscillations

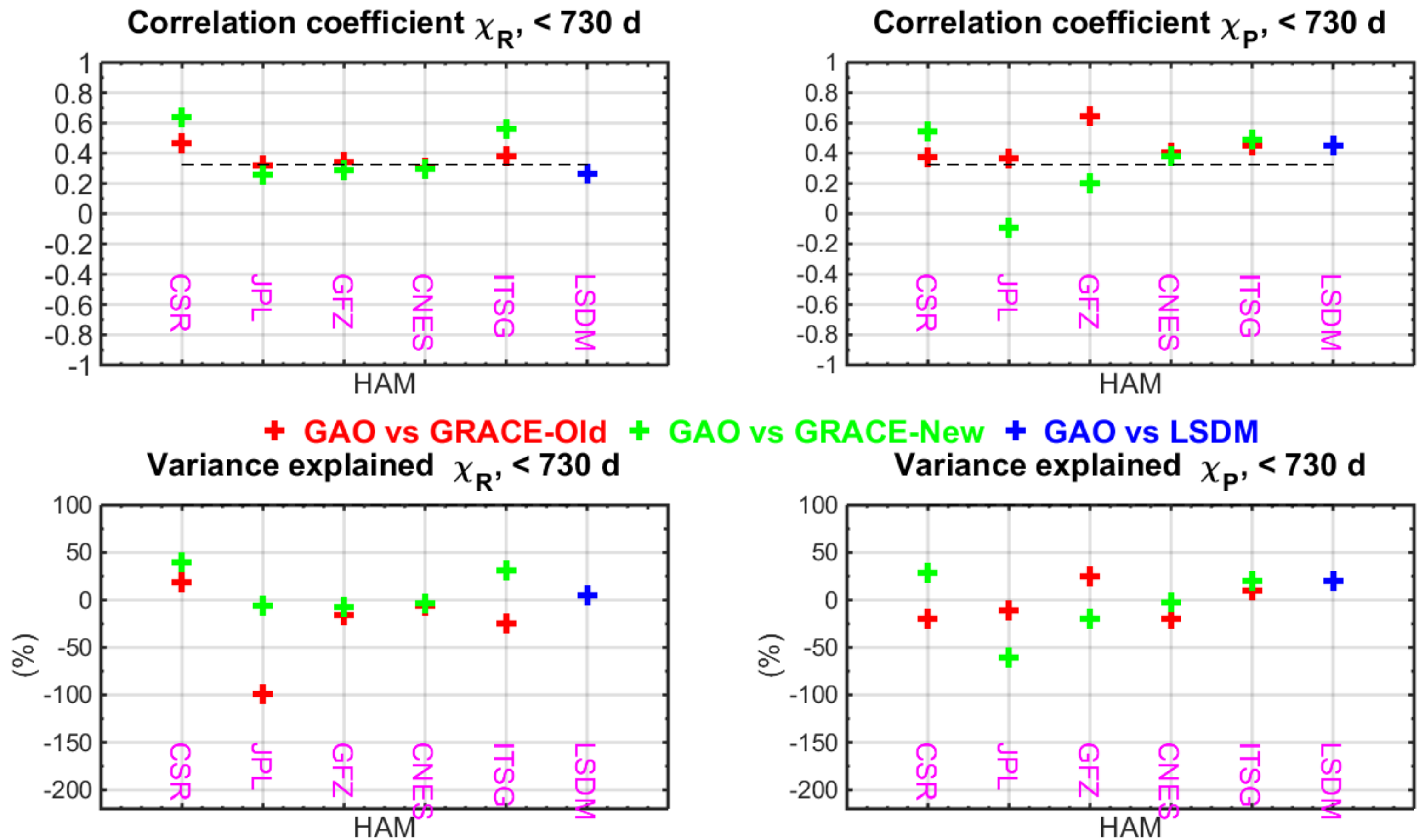

Fig. 11. Correlation coefficients of retrograde and prograde parts of short–term (periods <730 days) non–seasonal variation between GAO and HAM computed from GRACE solutions and LSDM model (with SLAM added); percentage of variance in GAO explained by HAM functions. The critical value of the correlation coefficient for 25 independent points and a confidence level of 0.95 is equal to 0.34. A standard error of a difference between two correlation coefficients for 25 independent points is equal to 0.30

Non-seasonal long-term oscillations

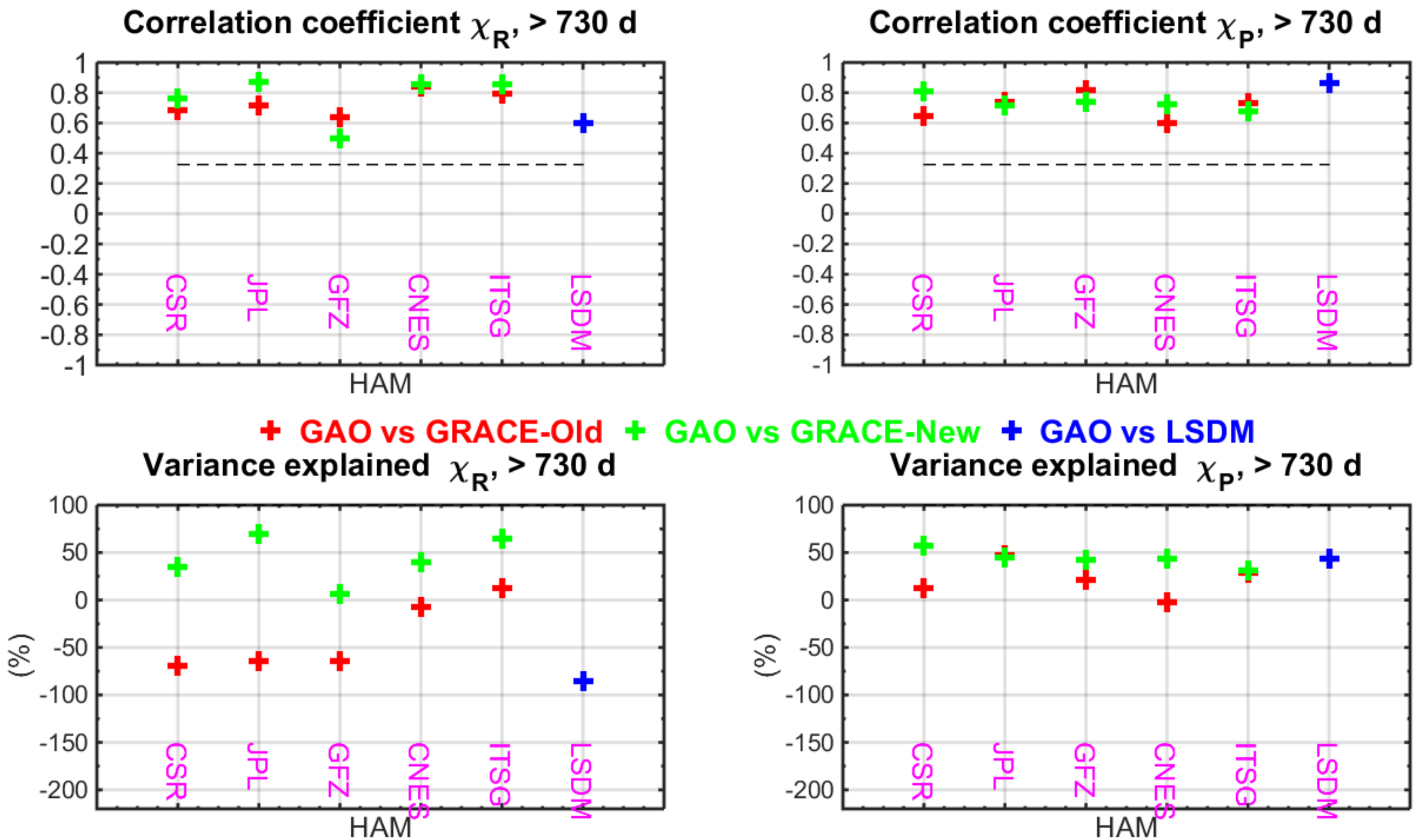

Fig. 12. Correlation coefficients of retrograde and prograde parts of long–term (periods >730 days) non–seasonal variation between GAO and HAM computed from GRACE solutions and LSDM model (with SLAM added); percentage of variance in GAO explained by HAM functions. The critical value of the correlation coefficient for 25 independent points and a confidence level of 0.95 is equal to 0.34. A standard error of a difference between two correlation coefficients for 25 independent points is equal to 0.30

Mean correlation and variances

Table 1. (a) Mean values of correlation coefficients between GAO and GRACE–based HAM for each oscillation considered: mean GRACE old (the mean of correlations for CSR RL05, JPL RL05, GFZ RL05, CNES RL03, ITSG 2016), mean GRACE new (the mean of correlations for CSR RL06, JPL RL06, GFZ RL06, CNES RL04, ITSG 2018). **(b)** Mean values of percentage variances in GAO explained by GRACE–based HAM for each oscillation considered.

Correlation coefficients and relative explained variance for HAM from LSDM model (with SLAM added) were added for comparison.

(a)	Mean correlation coefficients							
Series	seasonal		non–seasonal		non–seasonal short		non–seasonal long	
	χ_R	χ_P	χ_R	χ_P	χ_R	χ_P	χ_R	χ_P
mean GRACE old	0.47	0.44	0.47	0.57	0.36	0.45	0.73	0.71
mean GRACE new	0.58	0.53	0.52	0.53	0.41	0.30	0.77	0.73
LSDM	0.74	0.11	0.35	0.64	0.26	0.45	0.60	0.86

(b)	Mean relative explained variance (%)							
Series	seasonal		non–seasonal		non–seasonal short		non–seasonal long	
	χ_R	χ_P	χ_R	χ_P	χ_R	χ_P	χ_R	χ_P
mean GRACE old	12	7	–27	4	–25	–3	–38	21
mean GRACE new	25	24	19	18	11	–7	43	44
LSDM	54	–25	–19	29	5	20	–86	43

Summary and conclusions

- Here, we showed an alternative method of presenting hydrological polar motion excitation function. Instead of the use of two equatorial components of HAM which are directed towards Greenwich Meridian (χ_1) and 90°E meridian (χ_2), we decomposed χ_1 and χ_2 into prograde and retrograde circular terms (χ_P and χ_R), using for this purpose Complex Fourier Transform.
- We evaluated χ_P and χ_R components of HAM obtained from GRACE RL05 and RL06 series and from LSDM hydrological model by comparing them with hydrological signal in observed PM excitation (GAO).
- In contrast to χ_1 and χ_2 representation, where we observed significantly better results for χ_2 than for $\chi_1$component, the correlation and variance agreement with GAO was at the similar level for both χ_R and χ_P.
- The consistency in results between prograde and retrograde terms increased with the new GRACE solutions.

Summary and conclusions

- Despite different methods of representation, our general remarks are congruous with those obtained in similar works dedicated to χ_1 and χ_2 analyses:
  - ✓ With the new GRACE data, the consistency between different solutions has been increased.
  - ✓ HAM from the new RL06 GRACE data are more smoothed (smaller amplitudes and standard deviation) compared to HAM from RL05.
  - ✓ The new GRACE solutions provide better correlation and variance agreement with observed PM excitation than the previous GRACE data.
  - ✓ Despite improved correlation agreement with reference data, there is still no satisfactory amplitude and variance compatibility.
  - ✓ The level of agreement between HAM and GAO depended on oscillation considered and was higher for long–term variations than for short–term ones.
  - ✓ For most of the oscillations considered, the highest agreement with reference data was obtained for CSR RL06 and ITSG 2018 solutions. The highest results improvement was detected for JPL.
- The HAM function obtained from LSDM model processed by the GFZ, revealed a significant correlation with GAO for non-seasonal prograde and seasonal retrograde terms.

Thank you